2194 *Biochemistry* **2010,** *49,* 2194–2204
DOI: 10.1021/bi9017522

BIOCHEMISTRY
including biophysical chemistry & molecular biology
Article

Structure and Function of the Universal Stress Protein TeaD and Its Role in Regulating the Ectoine Transporter TeaABC of *Halomonas elongata* DSM 2581^{T†}

Eva S. Schweikhard,[‡,⊥] Sonja I. Kuhlmann,[‡,⊥] Hans-Jörg Kunte,[§,∥] Katrin Grammann,[∥] and Christine M. Ziegler*[,‡]

[‡]*Department of Structural Biology, Max Planck Institute of Biophysics, Max-von-Laue-Strasse 3, 60438 Frankfurt am Main, Germany,* [§]*Biology in Materials Protection and Environmental Issues, Federal Institute for Materials Research and Testing (BAM), Unter den Eichen 87, 12205 Berlin, Germany, and* [∥]*Institute for Microbiology and Biotechnology, University of Bonn, Meckenheimer Allee 168, 53115 Bonn, Germany* [⊥]*Both authors have equally contributed to the work*

Received October 11, 2009; Revised Manuscript Received January 10, 2010

ABSTRACT: The halophilic bacterium *Halomonas elongata* takes up the compatible solute ectoine via the osmoregulated TRAP transporter TeaABC. A fourth *orf* (*teaD*) is located adjacent to the *teaABC* locus that encodes a putative universal stress protein (USP). By RT-PCR experiments we proved a cotranscription of *teaD* along with *teaABC*. Deletion of *teaD* resulted in an enhanced uptake for ectoine by the transporter TeaABC and hence a negative activity regulation of TeaABC by TeaD. A transcriptional regulation via DNA binding could be excluded. ATP binding to native TeaD was shown by HPLC, and the crystal structure of TeaD was solved in complex with ATP to a resolution of 1.9 Å by molecular replacement. TeaD forms a dimer−dimer complex with one ATP molecule bound to each monomer, which has a Rossmann-like α/β overall fold. Our results reveal an ATP-dependent oligomerization of TeaD, which might have a functional role in the regulatory mechanism of TeaD. USP-encoding *orf*s, which are located adjacent to genes encoding for TeaABC homologues, could be identified in several other organisms, and their physiological role in balancing the internal cellular ectoine pool is discussed.

The halophilic proteobacterium *Halomonas elongata* can tolerate salt concentrations well above 100 g/L (1.72 M) NaCl (*1*). To avoid dehydration in such environments and to maintain an osmotic equilibrium, *H. elongata* amasses internally large quantities of compatible solutes. These highly water-soluble molecules do not disturb the cell metabolism even at molar concentrations and are used for osmoregulation by diverse groups of bacteria originating from various environments (*2*). A clear trend was observed in which the least salt-tolerant organisms synthesize disaccharides for osmoregulation, whereas marine (halotolerant) species accumulate sugar polyols, and halophilic bacteria employ nitrogen containing compatible solutes such as glycine betaine and ectoine (*3*, *4*). *H. elongata* synthesizes ectoine as its main compatible solute (*5*) but does not rely only on *de novo* synthesis. It can also take up ectoine from the medium. *H. elongata* is equipped with only one ectoine-specific transporter TeaABC (*6*), which was shown to be a new type of osmoregulated transport system belonging to the family of tripartite ATP-independent periplasmic transporter (TRAP-T) (*6*) evolutionarily placed between the families of secondary and ABC transporters. The key distinguishing feature of TRAP transporters is the presence of a periplasmic substrate binding protein (SBP) as found in ABC systems, but with transport being driven by an electrochemical ion gradient as found in secondary transporters. TRAP-Ts have two integral membrane subunits, a 12 TM helix subunit (TeaC) that probably harbors the substrate and ion binding sites and a 4 TM helix protein (TeaB) of unknown but essential function. These subunits can also be found as a single fused protein (*7*). The physiological role of TeaABC is not only to import exogenous ectoine from the environment but also to salvage endogenous ectoine leaking through the cytoplasmic membrane, which would be otherwise lost to the medium (*6*).

A 15.5 kDa universal stress protein (USP)[1] encoding *orf* of 441 bp was found immediately downstream of *teaC* (*6*) and was named *teaD* accordingly. Genes encoding homologues of USPs adjacent to a transporter have been observed not only in TRAP systems (*7*) but also for a wide range of secondary transporter and channel genes (*8*), but their role in transport has not yet been explored (*8*). This might also be related to the fact that although USPs form an ancient and conserved family of proteins found in all kingdoms of life (*9*), their biochemical activities and functional mechanisms are still not fully understood (*10*). USPs were separated into two classes depending on their capability to bind ATP (*11*). Many of the USPs are expressed in response to stress, such as starvation, oxidative stress, or DNA damage (*12*). Genes of ATP-binding USPs are sometimes located in the same operon together with genes encoding transporters (*13*), and it was suggested that these USPs sense internal energy pools to regulate transporter activity (*13*).

Here, we report on the function of the TRAP-T-associated USP TeaD. Our study reveals that TeaD regulates the internal ectoine concentration in *H. elongata* upon hyperosmotic stress. We have determined the crystal structure of TeaD in complex with ATP to 1.9 Å resolution. Furthermore, we could show that dimeric TeaD sequesters ATP during expression and that additional ATP stabilizes a dimer−dimer complex of TeaD. We discuss a regulatory mechanism of TeaD on the ectoine transport by TeaABC in *H. elongata*, which we extend based on genome sequence analysis to other high-affinity TRAP transporters with different substrate specificity.

[†]The work was funded by DFG KU 1112/3-1 and ZI 572/4-1.

*To whom correspondence should be addressed. Telephone: +49 (69) 6303-3054. Fax: +49 (69) 6303-3002. E-mail: christine.ziegler@mpibp-frankfurt.mpg.de.

 Published on Web 01/29/2010

MATERIALS AND METHODS

Bacterial Strains and Growth Conditions. Cells of *H. elongata* DSM 2581^T (DSMZ, Braunschweig, Germany) and *H. elongata* mutant strains KB1 (Δ*ectA*), KB1-3 (Δ*ectA*, Δ*teaA*), KB1-5 (Δ*ectA*, Δ*teaD*), and AFE (*ectC*::Tn*1732*) were grown aerobically at 30 °C on mineral salt medium MM63 with glucose as carbon source. For analysis by chromatography and nucleic acid isolation cells were grown in 100 mL of saline MM63 liquid medium contained in 250 mL flasks.

RNA Isolation. For RNA isolation, exponentially growing cells were harvested by centrifugation, and 100 mg wet cell mass was resuspended in 4 mL of buffer (50 mM sodium acetate, 10 mM EDTA) containing 0.5 mL of SDS (10%). After addition of 5 mL of hot phenol, the sample was incubated at 65 °C for 4 min and then frozen in liquid nitrogen. The frozen sample was thawed (37 °C) and centrifuged (2700*g*) to enhance phase separation. The top layer was removed and mixed with an equal volume of phenol/chloroform/isoamyl alcohol. After centrifugation at 8000*g* (5 min, 4 °C), the aqueous top layer was transferred to a microfuge tube, and RNA was precipitated in the cold (−70 °C). The precipitated RNA was further purified using the RNeasy kit from Qiagen (Germany) according to the manufacturer's instruction.

RNA Hybridization Experiment. For the construction of a *teaA*-specific RNA antisense probe, an intragenic *teaA* DNA fragment was PCR-amplified from *H. elongata* DSM 2581^T genomic DNA using a reverse primer (5′-ggatcctaatacgactcactatagggctcgccggtcatttcgat-3′), which carried the promoter sequence for T7 RNA polymerase. The DNA template was applied to *in vitro* transcription (2 h, 37 °C) to generate DIG-11UTP-labeled antisense *teaA* RNA. Influence of TeaD on the transcription of *teaA* was tested by RNA hybridization experiments using the DIG-labeled *teaA* antisense RNA. For that purpose, 0.5 μg of total RNA was transferred onto a nylon membrane using a vacuum slot-blot apparatus (Consort NV, Turnhout) and cross-linked by UV irradiation. Probe hybridization and chemiluminescence detection were carried out according to the DIG application manual (Roche Molecular Biochemicals, Germany). Chemiluminescence was detected by commercially available X-ray films or, in the case of a densitometric quantification, recorded with the help of a CCD camera (Fuji Luminescent Image Analyzer LAS-1000) and quantified using the software package Aida, version 2.11. To analyze the transcriptional organization of *teaABCD* by Northern hybridization, approximately 5 μg of total RNA was electrophoretically separated on a denaturing agarose gel (0.8%), transferred to a nylon membrane, and covalently bound to the membrane by UV irradiation. Bound RNA was hybridized with a DIG-labeled antisense *teaA* RNA probe for 12 h at 68 °C according to the DIG application manual (Roche Molecular Biochemicals, Germany). Probe hybridization was detected by chemiluminescence via X-ray film.

Promoter Mapping by 5′ RACE-PCR. To identify putative promoter sequences, the transcriptional initiation sites were mapped by a modified RACE-PCR procedure using RNA from exponentially growing cells adapted to 680 mM NaCl. Transcription initiation sites of *teaABCD* were mapped by generating cDNA using reverse transcriptase (Superscript III; Invitrogen, USA) and reverse primer RACE-teaA1 (5′-ccgaagcgatagacctgaac-3′). Applying terminal deoxynucleotide transferase, a poly-(C) tail was attached to the 3′ end, and the modified cDNA was PCR-amplified with forward primer AAP (abridged anchor primer; ggccacgcgtcgactagtacgggiigggiigggiig) from Invitrogen and reverse primer RACE-teaA2 (5′-aacggtatggtcggaattatc-3′). Finally, PCR-amplified cDNA was sequenced.

Determination of Cytoplasmic Ectoine by HPLC. For identification and quantification of intracellular ectoines, cells were harvested, freeze-dried, and extracted with methanol/chloroform/water as described by Galinski and Herzog (*14*). Cellular extracts containing water-soluble solutes were separated by isocratic HPLC on a NH_2 column using acetonitrile (80% v/v) as solvent. Eluted solutes were monitored with an UV detector at 220 nm.

Purification. The gene *teaD* was amplified from genomic DNA that was extracted from *H. elongata* (*15*), with the primers 5′-ggatgtaaggtcatatgttcaatcggatcatgg-3′ and 5′-cgggaagctttcagacgaccaggacggg-3′ using the GC-rich PCR system (Roche Applied Science, Germany). The PCR product was cloned into pET22b vector (Novagen, Germany) using the *Nde*I and *Hin*dIII restriction sites on vector and PCR product. The resulting vector pET22b::*teaD* was transformed into *Escherichia coli* host BL21-(DE3) (Novagen, Germany) for autoinduction protein expression (*16*). The LB medium preculture, which was grown for 6 h at 37 °C, was used to inoculate autoinduction medium. The recombinant TeaD protein was synthesized for 18 h at 28 °C. Cells were harvested by centrifugation at 5018*g* for 15 min at 4 °C and resuspended in 25 mM Tris, pH 7.5, and 150 mM NaCl. The crude cell extracts were disrupted in the cell disrupter (Constant Cell Disruption) and treated with DNase (Sigma-Aldrich, Germany) and 1 mM PEFABLOC protease inhibitor (Biomol, Germany). After centrifugation (140000*g*, 1 h at 4 °C), the supernatant was incubated in batch overnight with 10 mL of preequilibrated (25 mM Tris, pH 7.5, 150 mM NaCl) cation-exchanger Sepharose (SP-Sepharose Fast Flow; GE Healthcare, USA). After washing with 25 mM Tris, pH 7.5, and 250 mM NaCl, TeaD was eluted by a gradient against 1 M NaCl and immediately dialyzed against 25 mM Tris, pH 7.5, and 250 mM NaCl to remove high salt concentration. The sample was loaded onto a Superdex 75 10/300 GL (GE Healthcare, GE Healthcare Akta-Explorer 10) in 25 mM Tris, pH 7.5, 500 mM NaCl, and optional 600 nM and 2.5 mM ATP. Buffer exchange was carried out on a PD10 column (GE Healthcare, USA) with 25 mM Tris, pH 7.5, and 150 mM $MgCl_2$. The protein was directly used for crystallization or flash frozen in liquid nitrogen at −80 °C.

Determination of ADP/ATP with HPLC and ATPase Activity. To determine ATP-binding via HPLC (high-performance liquid chromatography), TeaD was purified via size exclusion chromatography against 25 mM Tris, pH 7.5, and 500 mM NaCl; afterward, the protein sample was denatured (2 min, 95 °C), followed by centrifugation (1 min, 13000*g*). Nucleotides in the supernatant were then analyzed by HPLC using a Spherisorb ODS (octadecyl-SiO_2)-1 column (Phenomenex, USA). A buffer containing 100 mM potassium phosphate, pH 6.4, 10 mM tetrabutylammonium bromide, and 7.5% acetonitrile was used as mobile phase. The detection occurred at absorption of 254 nm. The C-18 column was calibrated with a nucleotide ATP−ADP standard. ATPase activity of tetrameric TeaD was measured as described (*16*). Therefore, 10 μL of a 250 mM ATP solution was mixed with 10 μL of TeaD of 10 mg/mL. The reaction was started by adding 25 μL of 10% LDAO. The decrease in NADH concentration was monitored at 340 nm (Cary WIN UV; Varian, Germany) at 30 °C.

Blue Native Gel Electrophoresis. Purified protein was mixed with Native PAGE 4× Sample buffer (Invitrogen, USA)

and loaded onto a 4−16% polyacrylamide gradient gel (Invitrogen, USA). A mixture of seven different proteins was used as a standard: IgM pentamer (1048 kDa), apoferritin band I (720 kDa), apoferritin band II (480 kDa), B-phycoerythrin (242 kDa), Lactate dehydrogenase (146 kDa), bovine serum albumin (66 kDa), soybean trypsin inhibitor (20 kDa) (Native Mark Unstained Protein Standard Invitrogen, USA).The anode buffer contained 50 mM Bis-Tris, pH 7, and 50 mM Tricine, 15 mM Bis-Tris, pH 7, and 0.02% Coomassie G-250 was used as cathode buffer. The blue native PAGE was performed for 30 min at 80 V and 4 h at 200 V at 4 °C and fixed with a mixture of 10% acetic acid and 10% ethanol.

Crystallization. Crystals of TeaD were grown at 18 °C by the conventional hanging drop vapor diffusion method. The hanging drops of 300 nL size contained 4 mg/mL protein. Five millimolar ATP was added prior to crystallization. The mother liquor consisted of 100 mM Tris, pH 7.5, 200 mM $(NH_4)_2SO_4$, and 15% polyethylene glycol (PEG) 3350. The crystals typically grew to dimensions of 0.4 mm × 0.1 mm × 0.1 mm within 7−10 days. The crystals were washed in mother liquor and flash-frozen in liquid nitrogen before exposure to X-ray.

Data Collection, Structure Determination, and Refinement. All diffraction data were collected at beamline PXII at the Swiss Light Source (SLS). The data were reduced and scaled with the programs XDS and XSCALE (*17*). Initial phases were gained by molecular replacement with a polyglycine model of the structure of an USP of *Thermus thermophilus* (PDB code 2z09), available at the Protein Data Bank (http://www.rcsb.com) with the program PHASER (*18*) of the CCP4i suite (*19*); 64% of the sequences were docked in the initial map by ARP/wARP (*20*). Iterative rounds of manual building in COOT followed by refinement with REFMAC5 (*21*) including NCS and TLS were used to improve the initial model. NCS (noncrystallographic symmetry) was defined for the four chains in the asymmetric unit excluding the two flexible regions of the protein (residues 40−64 and 131−147). For TLS (translation screw libration) refinement each chain was divided into four groups, which were determined by TLSMD (*21*, *22*). All molecular drawings were produced with PYMOL (*23*).

Sequence and Structure Alignments. A search for similar structures of TeaD was done with DALI (*24*). Structural alignments were performed with TCOFFEE (*25*). Sequences of similar USPs were found with BLAST (*26*) and aligned with ClustalW (*27*). Sequence alignment was drawn with BioEdit (*28*) and ESPript (*29*).

RESULTS AND DISCUSSION

teaD Is Cotranscribed along with teaABC. To analyze the transcriptional organization of the *teaABCD* locus (Figure 1A), total RNA from *H. elongata* cells grown in minimal medium containing 690 mM NaCl was isolated and applied to Northern hybridization and RT-PCR experiments. Gene *teaA*, which encodes the substrate binding protein (SBP), can be transcribed separately from *teaABCD*, being the major transcript of the *teaABCD* cluster as shown by Northern hybridization (Figure 1B). Furthermore, the analyses revealed that *teaABC* is transcribed together with the *orf teaD* located downstream of *teaC* (Figure 1C). A similar transcription pattern was found for the TRAP transporter genes *dctPQM* from *Rhodobacter capsulatus*, where the SBP encoding *dctP* is also the abundant transcript when compared to the *dctPQM* mRNA (*11*). The increased mRNA level for the SBP is caused by the location of *teaA* and *dctP*, respectively, at the 5′-end of their corresponding gene

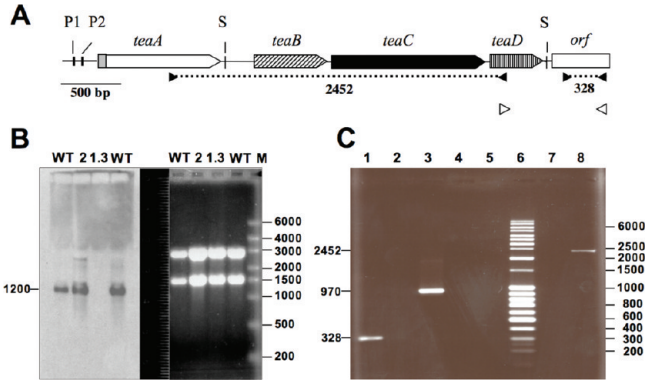

FIGURE 1: (A) Genetic and physical organization of the *teaABCD* locus. The transcription initiation sites were mapped by 5′ RACE-PCR, and inspection of the DNA sequences upstream of the initiation sites revealed the presence of a σ^{70}-dependent promoter (P1) and a σ^{S}-dependent promoter (P2). (B) Total RNA from *H. elongata* was separated by agarose gel electrophoresis (B II) and transferred onto a nylon membrane (B I). Northern blot analysis of RNA from *H. elongata* wild type (WT), ΔteaC mutant KB2 (*2*), and the teaA deletion mutant KB1-3 (1.3) was carried out using a teaA-specific RNA probe (B I). A single transcript of approximately 1.2 kb corresponding to the calculated size of a *teaA* transcript was detected by hybridization with the WT RNA, while no hybridization signal was detectable with the RNA of control strain KB1-3 (Δ*teaA*). (C) RT-PCR analysis of *teaABCD* proving that *teaD* is cotranscribed along with *teaABC*. A 2400 bp PCR product was amplified from cDNA and separated by agarose gel electrophoresis (lane 8), which matched the size of the calculated *teaABCD* PCR product (2452 bp). cDNA synthesized from *orf* was only detectable by PCR with forward and reverse primers binding inside *orf* (lane 1) but not if the corresponding forward primer (white right-pointing arrowhead in Figure 1A) was binding to *teaD* (lane 4), proving that *teaABCD* transcription is terminated behind *teaD*. The same primers (lane 4) led to a *teaD-orf* PCR product only if chromosomal DNA was used as template (lane 3, positive control). No DNA was amplified with the primers used in lanes 1, 4, and 8 from purified total RNA prior to cDNA synthesis (lanes 2, 5, and 7, negative control), proving that the *teaABCD* (*8*) and *orf* (*1*) products were indeed amplified from cDNA and not from contaminating chromosomal DNA. Key: S, stem−loop; P1, P2, promoter; left-pointing arrowheads, forward primers for PCR; right-pointing arrowheads, reverse primers for cDNA synthesis and PCR (white arrowheads stand for no PCR product and black arrowheads for DNA amplified); > · · · <, PCR product.

cluster in combination with a termination sequence following *teaA* and *dctP*. To allow for the transcription of the entire *teaABCD* gene cluster, an imperfect transcriptional terminator sequence is located between *teaA* and *teaB*. The stem−loop structure of *teaA* is followed by an AGTT GTTT sequence. A similar repeated CTTT motif has been found at the stem−loop structure of DctP (and other *R. capsulatus* operons) and is thought to act as a partial termination sequence (*11*), permitting read-through into genes *dctQ* and *dctM* coding for the membrane proteins (*11*). However, the transcript of the *tea* locus comprises not only the genes for the transporter proteins but also *teaD*, an *orf* coding for a putative USP. Interestingly, deletion of *teaD* resulted in a mutant strain of *H. elongata* that grew as well as the wild type, when the cells had to transport ectoine from the medium for osmoregulation (*6*). To clarify the function of *teaD*, we examined the uptake of ectoine via TeaABC in more detail.

TeaD Is a Negative Regulator on the Activity of TeaABC. To examine the role of *teaD* and the TeaD protein in ectoine transport via TeaABC, ectoine uptake following osmotic upshift was determined (Figure 2A). While *H. elongata* strain KB1 missing the ectoine synthesis gene (Δ*ectA*) accumulates 0.41 μmol of ectoine (mg of protein)$^{-1}$ in 60 min following upshock by the

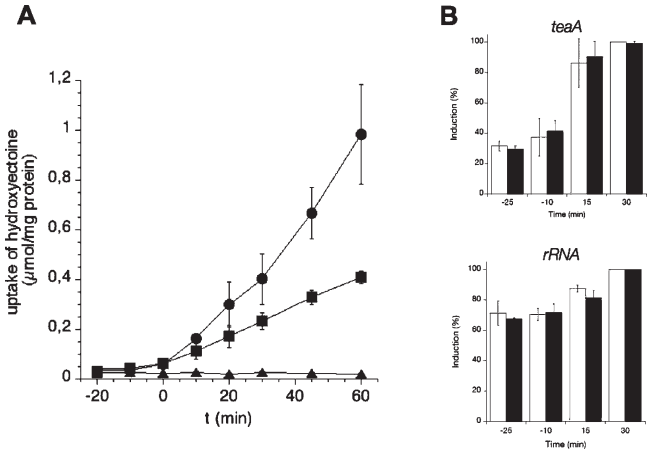

FIGURE 2: (A) Cells of *H. elongata* KB1 (Δ*ectA*), strain KB1-5 (Δ*ectA*, Δ*teaD*::Ω), and transport mutant AFE35 (Δ*ectA*, *teaC*::Tn*1732*) were grown in minimal medium MM63 containing 170 mM NaCl and 1 mM hydroxyectoine. At time zero, cells were exposed to osmotic stress by increasing the salt concentration to 690 mM, inducing osmoregulatory uptake of ectoine via TeaABC. The uptake of hydroxyectoine was monitored for 60 min by analyzing the cytoplasm of KB1, KB1-5, and AFE35 by HPLC with a UV detector. At minimum, all experiments were carried out three times. Symbols: ●, KB1-5; ■, KB1; ▲, AFE35. (B) Changes in *teaA* transcript level of *teaD* mutant KB1-5 (black bars) and *teaD*$^+$ strain KB1 (white bars) in response to hyperosmotic shock. Cells were grown in minimal medium containing 170 mM NaCl. In exponential growth phase salinity was increased to 680 mM NaCl. At 25 and 10 min before hyperosmotic shock and 15 and 30 min after shock cells were harvested and RNA was isolated and transferred to a membrane. Membrane-bound RNA was hybridized with *teaA*-specific antisense RNA probe, and RNA−RNA hybridization was determined by chemiluminescence. An antisense 16S rRNA probe was used as control. Emitted light was recorded by camera and quantified. Highest signal intensity was set to 100%.

TeaABC system, the *teaD* mutant *H. elongata* KB1-5 transported 0.95 μmol of ectoine (mg of protein)$^{-1}$, exceeding the ectoine level of the *teaD*$^+$ cells by more than 2-fold. The knockout of *teaD* had no obvious phenotypic effect and did not hamper growth of *H. elongata* KB1 at elevated salinity. It was proposed earlier that USPs contain DNA-binding motifs (*30*). To test whether TeaD is a DNA-binding protein and involved in transcriptional regulation of the *tea* locus, we quantified the *teaA* transcript in *teaD*$^+$ and *teaD* mutant strains. *H. elongata* KB1 and mutant strain KB1-5 (Δ*teaD*) were grown in minimal medium and exposed to sudden osmotic upshifts from 170 to 680 mM NaCl during exponential growth. Total RNA was isolated from cells before and after osmotic shock, and the mRNA of *teaA* was analyzed by dot RNA hybridization experiments (Figure 2B). The RNA hybridization experiments revealed that the *teaA* mRNA level increases in response to increasing osmolarity (approximately 70% increase). However, since the 16S rRNA is affected by the osmotic upshift as well (approximately 30% increase), it still has to be determined whether transcriptional overexpression alone or also a decrease in degradation of mRNA is the cause for the increase in mRNA. Importantly, the *teaA* mRNA level in the *teaD* knockout strain KB1-5 was identical to the *teaA* RNA content found in the *teaD*$^+$ strain KB1 (Figure 2B). On the basis of this result and the structural features of the TeaD protein presented below, we exclude a role of TeaD in transcriptional regulation of *teaABC*. Instead, we suggest that TeaD might act either as a translational regulator or as a direct or indirect regulator of TeaABC transport activity.

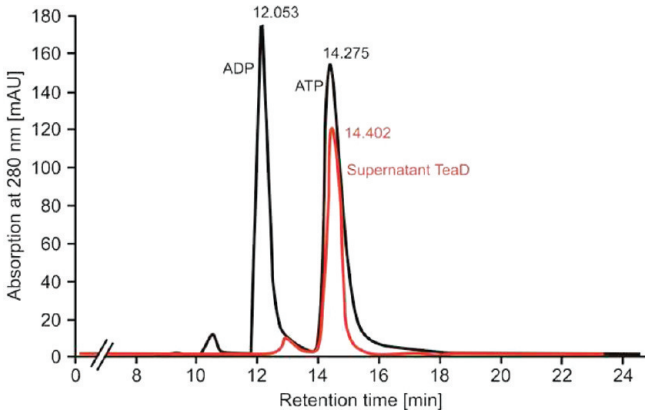

FIGURE 3: ATP binding of TeaD. ATP−ADP standards (black) are compared to the supernatant of denatured TeaD protein (red) on a high-pressure liquid chromatograph (HPLC). ADP has a retention time of 12 min and ATP 14.3 min. The supernatant of heat-shocked TeaD shows a retention peak at 14.4 min, which is comparable to the ATP standard.

TeaD Is an ATP-Binding Protein. The nucleotide-binding capacity of a subset of USPs was discovered when the structure of MJ0577, an USP from *Methanococcus jannaschii*, was solved in complex with ATP (*31*). A $GX_2GX_9G(S/T)$ motif was assigned for ATP binding in USPs (*11*). The presence of this motif in TeaD suggests its ATP-binding ability, which was examined by HPLC (Figure 3). TeaD was expressed in *E. coli* and purified to homogeneity by cation exchange (SP-Sepharose), subsequently followed by size exclusion chromatography (Superdex 10/300) against 25 mM Tris, pH 7.5, and 500 mM NaCl. Supernatants from boiled samples of TeaD were loaded onto the octadecyl-SiO_2 (ODS) C 18 Hypersil column. Compared to the ADP and ATP standards (Figure 3) the supernatant of denatured TeaD eluted always with ATP. We assume that TeaD binds ATP from its expression host *E. coli*. The association was sufficiently tight that nearly 35% of the nucleotide-binding sites were occupied upon purification assuming a 1:1 binding stoichiometry (ATP/monomer). However, a complete dissociation from TeaD could not be observed even after extensive washing steps during cation-exchange chromatography. TeaD was incubated with increasing ATP concentrations up to 10 mM ATP and investigated by HPLC, resulting in a dissociation constant of 0.8 μM for ATP binding. ADP was not present in the supernatants from boiled samples of TeaD, consistent with the fact that no ATPase activity could be detected for TeaD. However, TeaD might require an additional binding partner to hydrolyze ATP.

ATP-Dependent Tetramerization of TeaD. TeaD showed a tendency to form aggregates at concentrations above 2 mg/mL in the absence of 500 mM NaCl, which was an issue in crystallization. However, salt could be replaced by 2.5−5 mM ATP and 50−150 mM $MgCl_2$ to increase solubility of TeaD, suggesting a stabilizing effect upon ATP binding. Therefore, we investigated the aggregation/oligomerization behavior of TeaD dependent on the ATP concentration by size exclusion chromatography (SEC) and blue native (BN) gel electrophoresis.

SEC analysis (Figure 4A, red curve) of purified TeaD showed a monodisperse peak without aggregates (expected in the void volume at 8 mL), when 500 mM NaCl or 150 mM $MgCl_2$ was present in the running buffer, respectively. Compared to six standard proteins (Figure 4A, right) the elution volume corresponds to a TeaD dimer at 32 ± 3 kDa. However, incubation of TeaD with 2.5 mM ATP revealed the appearance of an additional

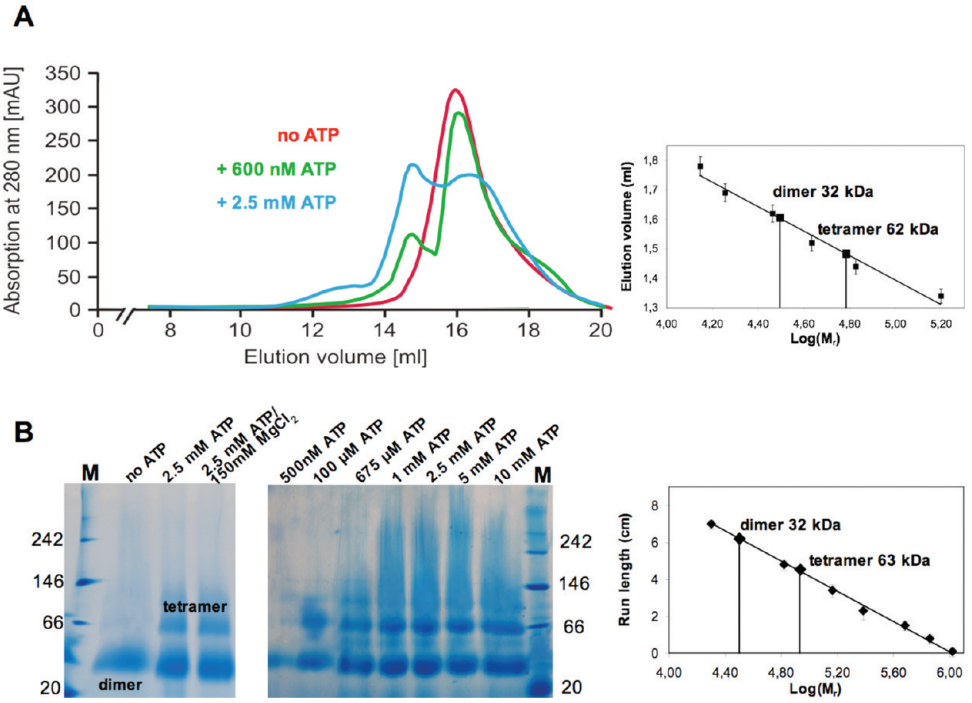

FIGURE 4: (A) Size exclusion chromatography of TeaD. TeaD eluted as a dimer in 25 mM Tris, pH 7.5, and 500 mM NaCl (red curve). A partial shift to tetramer could be observed when ATP was added to the gel filtration buffer depending on the ATP concentration (600 nM, green curve; 2.5 mM, blue curve). A calibration curve to determine the molecular mass was obtained from the six standard proteins: aldolase (158 kDa), albumin bovine from bovine serum (67 kDa), albumin from chicken egg (43 kDa), carboamylase (29 kDa), myoglobin equine from horse muscle (18 kDa), and ribonuclease (14 kDa). (B) Blue native PAGE (4−16%) of TeaD in the presence of varying amounts of ATP. The molecular masses of the standard proteins (M) are indicated on the left side. Lanes: (1) TeaD without ATP incubation, (2) TeaD incubated with 2.5 mM ATP, (3) TeaD incubated with 2.5 mM ATP and 150 mM $MgCl_2$, and (4−7) TeaD incubated with 500 nM, 100 μM, 675 μM, 1 mM, 2.5 mM, 5 mM, and 10 mM ATP, respectively. A calibration curve of the run length was determined using seven different proteins as a standard: IgM pentamer (1048 kDa), apoferritin band I (720 kDa), apoferritin band II (480 kDa), B-phycoerythrin (242 kDa), Lactate dehydrogenase (146 kDa), bovine serum albumin (66 kDa), soybean trypsin inhibitor (20 kDa) (Native Mark Unstained Protein Standard Invitrogen, USA).

higher oligomeric state (Figure 4A, blue curve). This state was assigned as a tetramer with a molecular mass of 62 ± 3 kDa according to the calibration curve. A tetrameric state, although with a lower occupancy (1:3) than the dimeric state, appeared already at a concentration of 600 nM ATP (Figure 4A, green curve). BN gel electrophoresis (Figure 4B) confirmed the dimeric state of TeaD (lane 1) by comparison to seven standard proteins (Figure 4B, right), with a molecular mass of 37 ± 3 kDa which is comparable to that determined by size exclusion chromatography. Upon incubation with 2.5 mM ATP (lane 2) and 150 mM $MgCl_2$/2.5 mM ATP (lane 3) a 1:1 distribution of dimers and tetramers (66 kDa) was also observed in the BN gel, suggesting that Mg^{2+}, which stabilizes TeaD at higher concentrations, does not play a role in TeaD tetramerization. Different ATP concentrations ranging from 500 nM to 10 mM (lanes 4 and 5) providing a 10−160-fold excess of ATP show that the ATP-saturated TeaD forms always a dimer−tetramer equilibrium with an apparent stoichiometry of 1:1.

Crystal Structure of TeaD: Tetrameric Assembly and ATP Binding. TeaD crystals grew in 100 mM Tris, pH 7.5, 200 mM $(NH_4)_2SO_4$, 15% polyethylene glycol (PEG) 3350, and 5 mM ATP. The crystals exhibit $P2_12_12_1$ symmetry. The structure of TeaD was solved by molecular replacement to 1.9 Å resolution. The final TeaD model has an R_{work} of 21% and an R_{free} of 25% (Table 1). The asymmetric unit in TeaD crystals comprises four tightly bound TeaD molecules (Figure 5A). The TeaD monomer consists of a five-stranded parallel β-sheet surrounded by five α-helices and binds one molecule of ATP (Figure 5B). The structure is resolved from residue 1 to residue 147 missing residues 42−46 and 57−60 (corresponding to α2 and η1) in monomers C and D and residues 123−129 of monomer C, suggesting that these are highly flexible regions. Monomer−monomer contacts (Figure 5B) are formed through hydrogen bonds involving the main chains of Val144 and Val146 and through hydrophobic interactions mediated by β-strand 5 and α-helix 5 with a buried surface of 3700 Å^2 between monomers A and B or monomers C and D (Figure 5B). The buried surface of the dimer−dimer contacts of 5770 Å^2 is build by α2 and η1. The dimer−dimer contact region of monomers B and D is shown in Figure 5C. The hydrogen bonds and their lengths are varying for each dimer−dimer contact region (D to B, A to C, C to A). However, the hydrogen bonds between Ser50 and Gly11 and between Ser48 and Lys13 are conserved throughout the tetrameric structure.

The TeaD protein possesses an ATP-binding Rossmann fold with alternating α-helices and β-strands. Details of hydrogen-bonding interactions are shown in Figure 6A,B. Interestingly, Arg135 is provided by a neighboring dimer and forms a hydrogen bond to the Pγ of ATP. Electron density observed close to the phosphate groups of each ATP was assigned as Mg^{2+}-ion based on its characteristic hexagonal coordination in the structure. Mg^{2+} was present during size exclusion chromatography and crystallization. The interaction of Mg^{2+} with the Pα and the Pβ of ATP is stronger than with the Pγ. In monomer D the Pγ is not coordinating the Mg^{2+}-ion. Three water molecules complete the octahedral coordination of the magnesium ion.

TeaD shares a common overall fold with other USPs (Table 2, Figure 7), which differ mainly in the poorly conserved regions α2 and η1. The short α2-helix observed in TeaD is also present in the structure of the eukaryotic USP of *Arabidopsis thaliana* (2dum),

Table 1: X-ray Data Collection, Refinement, and Model Statistics of TeaD

data collection		refinement	
unit cell (Å)	$a = 74.1, b = 74.7, c = 97.0$	resolution (Å)	1.9
space group	$P2_12_12_1$	R_{work} (%)	25.2
wavelength (Å)	0.9765	R_{free} (%)	21.9
resolution[a] (Å)	20−1.9 (1.95−1.90)	no. of protein atoms	4388
no. of obsd reflections[a]	208028 (11146)	no. of ATP atoms	124
no. of unique reflections[a]	42968 (3183)	no. of solvent molecules	97
completeness[a] (%)	99.8 (99.6)	no. of magnesium ions	6
I/σ(I)[a]	13.2 (2.2)	rmsd[c] from ideal bond length (Å)	0.006
R_{meas}[a,b] (%)	8.1 (73.4)	rmsd[c] from ideal bond angles (deg)	1.08
		average B factor model atoms (Å^2)	29.0
		Wilson B factor (Å^2)	40.4
		Ramachandran plot favored (%)	96
		Ramachandran plot allowed (%)	4

[a]Data in parentheses are for the highest resolution shell. [b]For definition of R_{meas}, see ref *38*. [c]Root mean square deviation. The fraction of R_{free} is 5% of the total reflections.

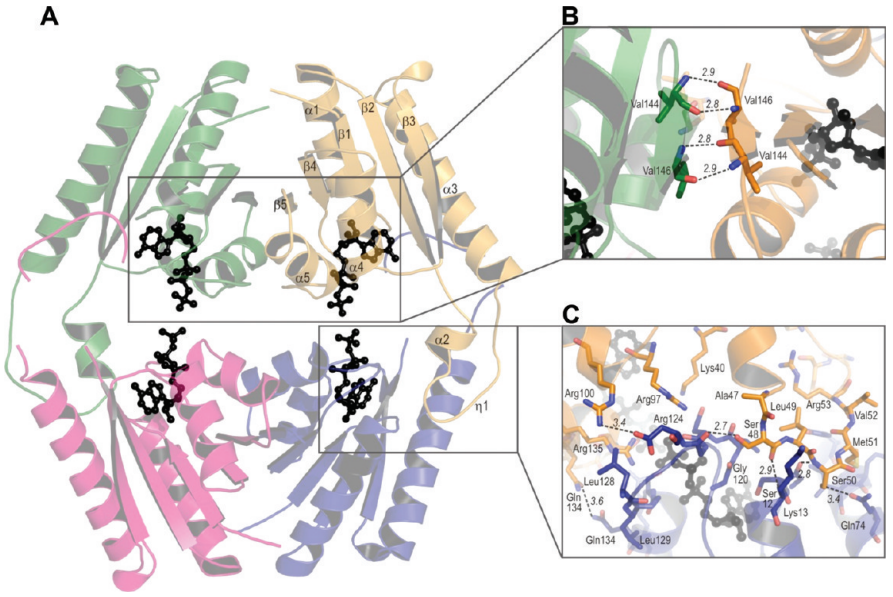

FIGURE 5: Overall structure of TeaD and dimer−tetramer contacts. (A) TeaD crystals have four tightly packed molecules in the asymmetric unit. A dimer of dimers is formed by interaction from one dimer (monomer A in green and B in yellow) with the other dimer. One ATP (black) is bound to each monomer exhibiting a Rossmann fold. (B) The dimer contacts are formed by β-sheet 5 and α-helix 4. The dashed lines and the numbers indicate the hydrogen bonds and their lengths. (C) The dimer−dimer contact region of monomers B and D. The main interactions are coordinated by α-helix 2 and the loop region η1.

as well as in the archaeal USPs from *Pyrococcus horikoshii* (2dum), *M. jannaschii* (1mjh), and *Aquifex aeolicus* (1q77), while no helical secondary structure element can be observed in that region in USPs of *Mycobacterium tuberculosis* (3cis) and *Archaeglobus fulgidus* (3dlo). Monomer−monomer interaction regions (α5 and β5) are highly conserved in all USPs, while a similar tetrameric assembly as in TeaD was observed only in crystal structures of the USP−ATP complexes from *T. thermophilus* (2z08), *M. jannaschii* (1mjh), *Klebsiella pneumoniae* (3fdx), and *M. tuberculosis* (3cis). The majority of USPs without bound ATP or in complex with ADP or AMP crystallizes as dimers. This indicates that an ATP-dependent formation of a dimer−dimer complex is found also in other USPs. A structural comparison reveals very similar coordination of ATP-binding. The ATP-binding residues are clustered in four areas (Figure 7). The highly conserved adenosine-binding residues are located between β1 and α1 (PVDXXSXGA 8−16, X indicating nonbinding residues), on β2 (LXV 36−38), and on α4 (P 98). The less conserved phosphate-binding residues IGXQGXNG 116−123 and GSVAXR 130−135 are on the loop between β4 and α5 (Figure 7). Together with TeaD (Figure 7), they all share the $GX_2GX_9G(S/T)$ sequence, which was defined as the ATP-binding motif for *M. tuberculosis* USPs (*12*). However, the USP from *K. pneumoniae* lacking the motif in its sequence was crystallized in complex with ADP (3fh0) and ATP (3fdx), showing that the absence of this motif is not a criterion to classify an USP as a non-ATP-binding USP. Interestingly, in the structures of TeaD and the USPs of *K. pneumoniae* and *T. thermophilus*, the binding of Pγ of ATP is mediated by a positively charged residue arginine or lysine of an adjacent dimer (Figures 6A,B and 7), reminiscent of the R-finger. The R-finger was described for ATPases (*32*) and the GTPase activating enzyme (GAP) in complex with Ras (*33*). The arginine is believed to compensate developing negative charges accumulating during phosphoryl transfer. Thus the transition state in ATP/GTP hydrolysis is stabilized and the hydrolysis is favored (*33*), which is enhanced by formation of a dimer of dimers, when Arg135 interacts with ATP. This finding suggests that TeaD and the other described USPs might have an ATPase activity. However, no ATPase activity could be detected for TeaD *in vitro*, indicating that there might be an additional reaction partner.

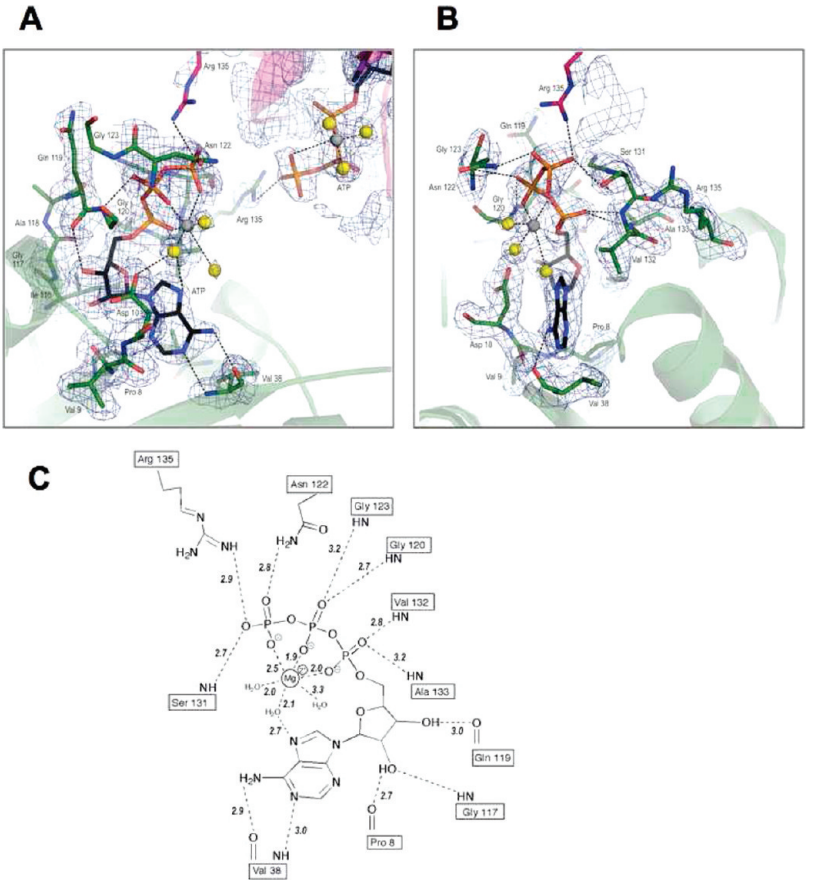

FIGURE 6: ATP-binding site. (A, B) Stick representation of ATP and the ATP-binding residues in two different views with oxygen in red and nitrogen in blue, while the phosphates of ATP are displayed in orange. A $2F_o - F_c$ omit map is shown for ATP (black), the Mg^{2+} ions (gray ball), and the water molecules (yellow balls), while a regular $2F_o - F_c$ map is drawn around the residues, which coordinate ATP binding. Arginine 135 of chain C (pink) binds to ATP in chain A (green) and vice versa. (C) Schematic drawing of the ATP-binding site in monomer A. The dashed lines indicate hydrogen bonds with their lengths and the coordination of the Mg^{2+} ion. CHEMDRAW was used to create this figure.

Table 2: Structures of USPs Available in the PDB Identified by a DALI Search against the TeaD Structure[a]

PDB-chain	*Z*	rmsd	lali	nres	%	organism	cofactor	protein
2z09-A	20, 2	1, 3	119	124	33	*T. thermophilus*	ACP	USP (Q5SJV7)
2z08-A	20, 0	1, 3	118	123	33	*T. thermophilus*	ATP	USP (Q5SJV7)
1wjg-A	19, 0	2, 0	126	135	31	*T. thermophilus*	no	USP (Q5SJV7)
3cis-C	18, 6	2, 1	134	290	21	*M. tuberculosis*	ATP	Rv2623
1mjh-A	18, 5	2, 5	135	143	28	*M. jannaschii*	ATP	MJ0577
3dlo-A	18, 2	2, 0	124	134	26	*A. fulgidus*	no	USP (O29432)
3fdx-A	17, 5	2, 1	124	127	28	*K. pneumoniae*	ATP	KPN_01443
3fh0-B	17, 5	2, 3	124	125	27	*K. pneumoniae*	ADP	KPN_01444
3fg9-E	16, 3	2, 2	129	150	23	*Lactobacillus plantarum WCFS1*	no	USP (Q88RY8)
2gm3-E	15, 1	3, 7	120	153	21	*A. thaliana*	AMP	USP (Q8LGG8)
2dum-C	15, 0	3, 4	137	146	26	*P. horikoshii*	no	PH0823
2pfs-A	14, 6	2, 4	117	125	27	*Neutrosomas europaea*	no	USP (Q82 VN8)
1jmv-C	13, 1	2, 5	115	133	22	*H. influenzae*	no	USP A
1tq8-A	12, 7	2, 3	99	127	25	*M. tuberculosis*	no	Rv1636
1q77-A	11, 5	3, 0	125	138	19	*A. aeolicus*	no	AQ_178

[a]rmsd (root mean square deviation) and the sequence identities (%) over a range of matching residues (lali) out of the total number of residues (nres) of 12 different USPs are summarized up to a significant *Z*-score of 10. The Uni-Prot accession numbers are given in parentheses.

Role of USPs in Specific Ectoine TRAP Transporters. A BLAST search for proteins that are related to the amino acid sequence of TeaD revealed a number of USPs of up to 58% sequence identity to TeaD. Nevertheless, only the first 12 hits comprise TeaD homologues, in the sense that they are organized in a common operon together with a TRAP transporter (Table 3), while USPs with sequence identities to TeaD below 43% were genetically not organized next to any TRAP-T system. All of these TeaD homologues stem from microorganisms that belong to the proteobacteria. They comprise the heterotrophic and phototrophic genera of the α-proteobacteria *Oceanibulbus*, *Fulvimarina*, *Rhodobacterales*, *Silicibacter*, *Oceanicola*, and *Roseobacter* sp. and genera of γ-proteobacteria *Oceanobacter*, *Marinobacter*, and *Reinekea*, of which *Oceanobacter* is the closest

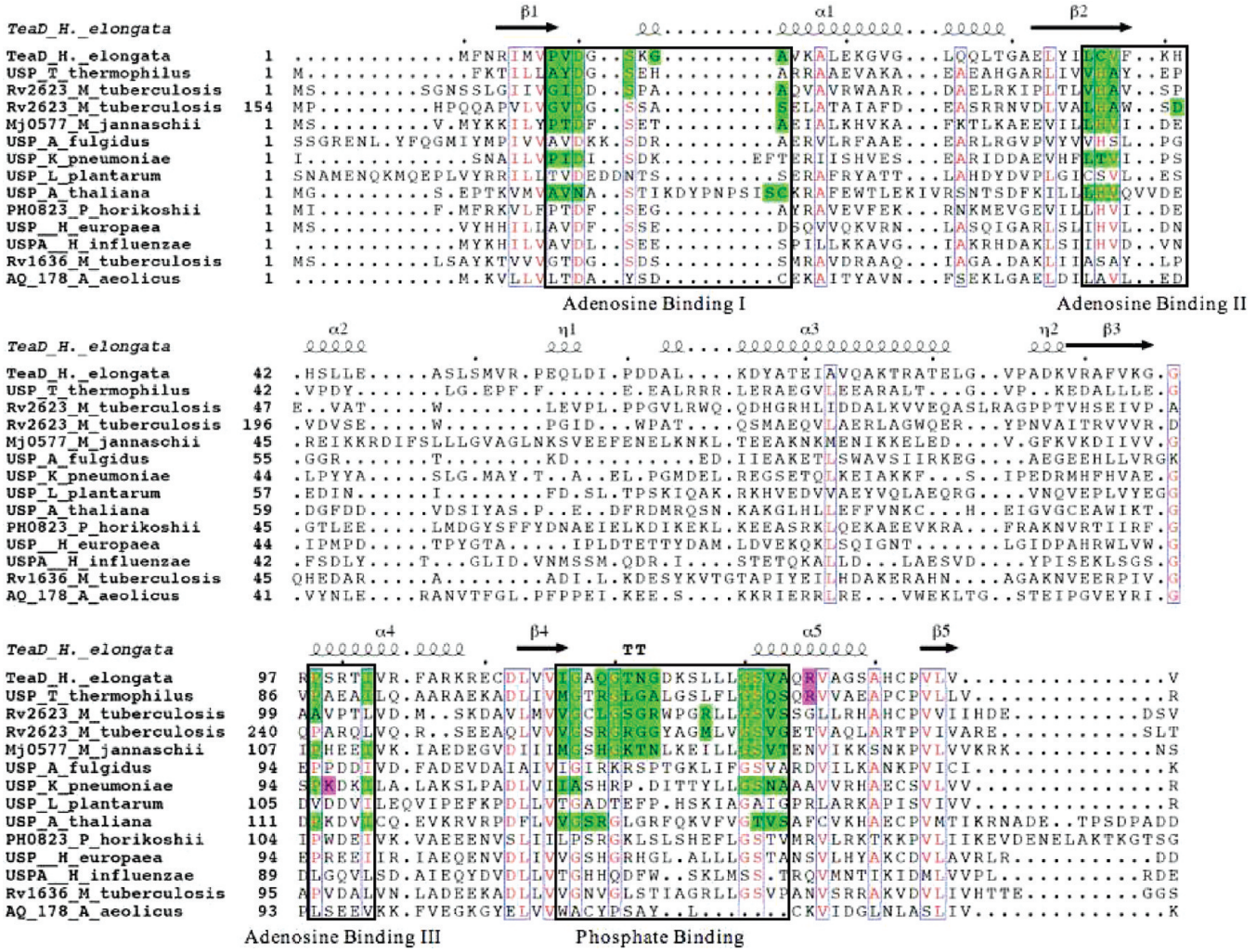

FIGURE 7: Sequence alignment, which resulted from a structural alignment of TeaD with structures of USPs available in the Protein Data Bank. The two USP domains of *M. tuberculosis* Rv2623 protein were examined separately. Residues that are conserved in at least 60% of all sequences are in red. All conserved residues are in blue boxes. ATP and, for *A. thaliana*, AMP interaction sites are highlighted in green. The R-finger arginine and the comparable lysine are highlighted in pink. The black boxes indicate the clusters of the ATP-binding residues.

Table 3: Level of Sequence Identity of 12 TeaABC Homologues[a]

	sequence identity to	TeaD (%)	TeaC (%)	TeaB (%)	TeaA (%)	no. of TRAP
	H. elongata	**100**	100	100	100	2
1	*Oceanobacter* sp.	**58**	78	66	72	1
2	*Marinobacter algicola*	55	84	71	78	6#
3	*Marinobacter hydrocarbonoclasticus*†	57	85	69	77	5#
4	*Marinobacter* sp.	54	83	69	74	6#
5	*Reinekea* sp.	51	83	68	74	4#
6	*Aurantimonas*	**52**	73	55	52	3
7	*Oceanibulbus indolifex*	48	75	60	57	10#
8	*Fulvimarina pelagi**	48	73	59	53	4#
9	*S. pomeroyi**	48	74	57	61	20#
10	*Oceanicola batsensis*	45	77	61	60	14#
11	*Roseobacter* sp. AzwK-3b	48	74	57	61	7
12	*Roseobacter* sp. SK209-2-6	**43**	74	59	59	12
	Vibrio sp.		64	49	40	3

[a]These transporters all possess a TeaD homologue encoding gene on their operon. There is an obvious gap in sequence identity of the whole TeaABC transporter when the TeaD homologue is missing as in *Vibrio*. A selection of USPs (indicated in bold letters) is shown in the sequence alignment in Figure 8. The total number of TRAP transporter systems and the existence of an ectoine synthesis pathway found in the respective organisms are as indicated: *, no ectoine synthesis; #, fragmented TRAP systems; †, formerly *Marinobacter aquaeolei*.

relative of *H. elongata*. All bacteria are living either in marine or in saline habitats. Regarding the salt requirement, *Marinobacter* species resemble *H. elongata* the most and display a similar salt tolerance (*34*). The 12 TeaD homologues (Table 3) show conserved ATP-binding sites and a high conservation in the flexible region of α2 and *η*1 (labeled green, Figure 8), which is the

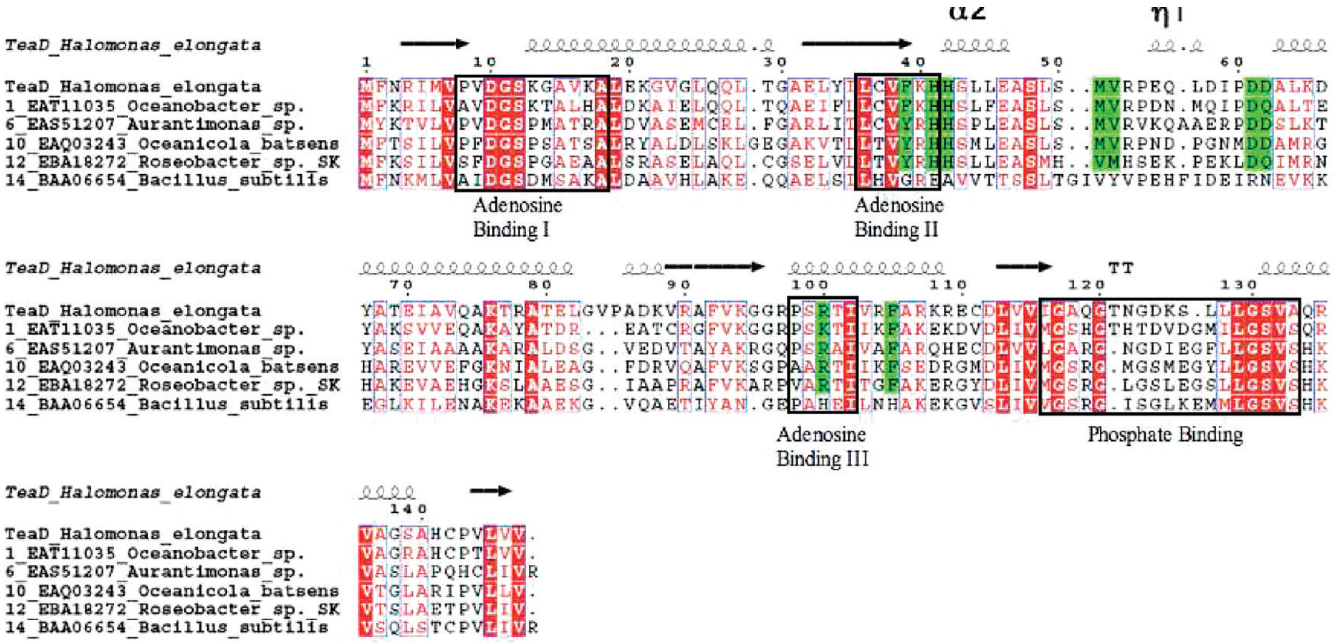

FIGURE 8: Sequence alignment TeaD against TeaD homologues originating from *Oceanobacter* sp. (58% sequence identity), *Aurantimonas* (52% sequence identity), *Oceanicola* (45% sequence identity), *Roseobacter* (43% sequence identity), and *B. subtilis* (37% sequence identity). All TeaD homologues are encoded by genes in close proximity of a TRAP transporter except the USP of *B. subtilis*, which is not related to a TRAP-T or a transporter.

tetramerization region in TeaD. To show the significance of this conservation, the USP from *Bacillus subtilis* was also included in the sequence alignment. This USP is not located next to a TRAP-T and is significantly different in these regions even though the overall sequence identity to TeaD is still 37%. The TeaD homologues show not only a sequence identity but also their associated TRAP-T proteins, which are corresponding to TeaABC from *H. elongata* (Table 3). Transporter proteins, which miss the USP-encoding sequence in their neighborhood, show a significant lower sequence identity. The decrease in sequence identity is very pronounced for the substrate binding proteins, i.e., TeaA homologues. Moreover, the ectoine-binding residues (*35*) Phe66, Trp167, and Trp188 are conserved in all 12 TeaA homologues (sequence identity > 52%) while they are not conserved in those TRAP transporters missing the USP gene. This suggests that these 12 proteins are specific ectoine-binding proteins, and the 12 corresponding TRAP systems probably have similar physiological properties to TeaABC. The conservation of TeaD in these systems indicates that these USPs play an important role together with the TRAP transporter in balancing the internal ectoine pool. TeaABC not only is required to accumulate external ectoine in response to osmotic stress but also functions as a salvage system for ectoine leaking out of the cell. This was found by analyzing strains of *H. elongata*, which possess an inoperable TeaABC transporter. These strains constantly excreted ectoine to the surrounding medium. Since uptake of compatible solutes from the medium via osmoregulated transporters will result in a decreased level of compatible solutes synthesized by the cell, it was suggested that TeaABC might be integrated (directly or indirectly) in the regulation of the cell's compatible solute synthesis (*6*). Ectoine release via mechanosensitive export channels and subsequent ectoine uptake via TeaABC could serve as a signal for regulating ectoine synthesis and degradation, respectively. Since TeaD is an ATP-binding protein, it is tempting to speculate whether TeaD is modulating the osmoregulatory uptake of ectoine according to the ATP status of the cell and thereby controlling the internal ectoine pool. However, the occurrence of TeaABCD-like TRAP systems is not always linked to the presence of an ectoine synthesis pathway. In fact, organisms such as *Silicibacter pomeroyi* are equipped with *teaABCD* but are missing the *ectABC* genes required for ectoine synthesis and do not use ectoine as a compatible solute. Instead, they carry the *eut* genes, which are thought to be involved in ectoine degradation (*36*), and can use ectoine as a nutrient.

Besides the TeaABC transporter, two more TRAP-Ts in *H. elongata* are linked to USPs. One is a TAXI TRAP-T (*13*) whose SBP shows a high degree of sequence identity to the glutamate/glutamine-binding protein from *T. thermophilus*, which structure was solved to 1 Å resolution (1US5). Similar glutamate transporters linked to USPs were found in several halophilic organisms, and each organism possesses a glutamate synthesis pathway. Glutamate plays an important role in osmotic stress response in *H. elongata*, because it is a counterion for K^+ ions, which are accumulated as osmolytes as a first response to hyperosmotic stress. In the moderately halophilic, chloride-dependent bacterium *Halobacillus halophilus* glutamate and glutamine are used as main compatible solutes at external salinities of 1.0−1.5 M NaCl, and biosynthesis of these solutes is regulated by chloride (*37*). Ectoine and glutamate are not the only osmoprotectants which are transported by a TRAP transporter linked to an USP. In *Roseobacter* species TRAP transporters associated to USPs were found which are specific for taurine (*7*), a compatible solute widespread among marine invertebrates. We assume that these three USPs are involved in the regulation of ectoine, glutamate, and taurine transport via TRAP transporters. All three show sequence conservation of several residues (magenta rhombi, Figure 9), but they differ significantly in their tetramerization region, which is located in α2, η1, and α3. It can be assumed that this region might be specifically involved in the regulatory interaction of the USP with the transporter itself or an additional interaction partner, and consequently the oligomerization interface has to be characteristic for the respective compatible solute

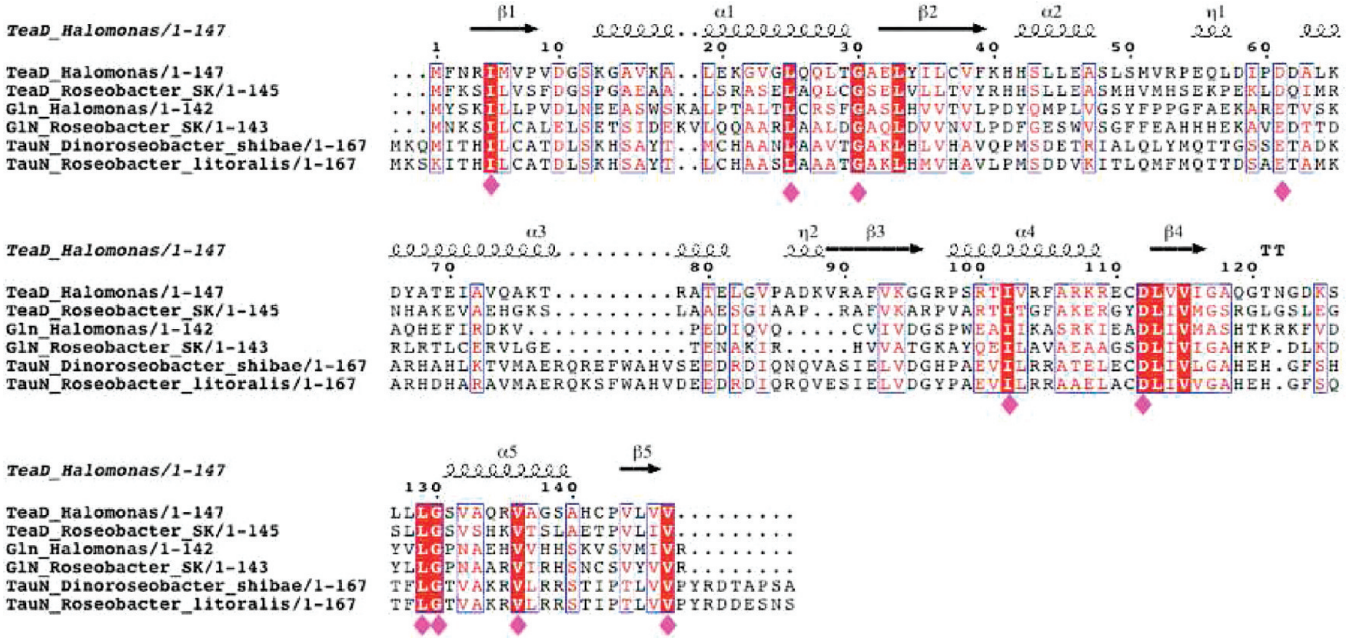

FIGURE 9: Pairwise sequence alignment of USPs associated to TRAP transporters involved in ectoine (TeaD), glutamate (Gln,) and taurine (TauN) transport. Magenta rhombi label conserved residues in all USPs.

transporter system. The regulatory mechanism could involve an association/dissociation of the dimer/ATP-bound tetramer. In the dimeric state, the highly protein-interactive regions in α2, α3, and β3 would be available for a specific regulatory interaction of the USP with the transporter or, e.g., with a protein of the respective synthesis/degradation pathway, while they would be unavailable for such an interaction in a tetrameric state. Up to now it can only be speculated that ATP binding switches these TRAP-T associated USPs in an interactive state, suggesting that the internal energy pool plays a role in transporter activation.

ACKNOWLEDGMENT

We thank Anke Terwisscha van Scheltinga (University of Groningen) and Özkan Yildiz (Frankfurt, MPI) for data collection and processing assistance, Karen Davies (Frankfurt, MPI) for important discussions, Helga Volk for help with the figures, and Stefan Köster (Frankfurt, MPI) for helpful discussions and support in purification and crystallization. We are grateful to the beamline staff at SLS PXII (Villigen, Switzerland) for excellent facilities and assistance.

REFERENCES

1. Goller, K., Ofer, A., and Galinski, E. A. (1998) Construction and characterization of an NaCl-sensitive mutant of *Halomonas elongata* impaired in ectoine biosynthesis. *FEMS Microbiol. Lett. 161*, 293–300.
2. Brown, A. D. (1976) Microbial water stress. *Bacteriol. Rev. 40*, 803–846.
3. Galinski, E. A., and Truper, H. G. (1982) Betaine, a compatible solute in the extremely halophilic phototropic bacterium *Ectothiorhodospira halochloris*. *FEMS Microbiol. Lett. 13*, 357–360.
4. Mackay, M. A., Norton, R. S., and Borowitzka, L. J. (1984) Organic osmoregulatory solutes in *Cyanobacteria*. *J. Gen. Microbiol. 130*, 2177–2191.
5. Wohlfarth, A., Severin, J., and Galinski, E. A. (1990) The spectrum of compatible solutes in heterotrophic halophilic *Eubacteria* of the family *Halomonadaceae*. *J. Gen. Microbiol. 136*, 705–712.
6. Grammann, K., Volke, A., and Kunte, H. J. (2002) New type of osmoregulated solute transporter identified in halophilic members of the bacteria domain: TRAP transporter TeaABC mediates uptake of ectoine and hydroxyectoine in *Halomonas elongata* DSM 2581(T). *J. Bacteriol. 184*, 3078–3085.
7. Mulligan, C., Kelly, D. J., and Thomas, G. H. (2007) Tripartite ATP-independent periplasmic transporters: application of a relational database for genome-wide analysis of transporter gene frequency and organization. *J. Mol. Microbiol. Biotechnol. 12*, 218–226.
8. Barabote, R. D., Tamang, D. G., Abeywardena, S. N., Fallah, N. S., Fu, J. Y., Lio, J. K., Mirhosseini, P., Pezeshk, R., Podell, S., Salampessy, M. L., Thever, M. D., and Saier, M. H., Jr. (2006) Extra domains in secondary transport carriers and channel proteins. *Biochim. Biophys. Acta 1758*, 1557–1579.
9. Drumm, J. E., Mi, K., Bilder, P., Sun, M., Lim, J., Bielefeldt-Ohmann, H., Basaraba, R., So, M., Zhu, G., Tufariello, J. M., Izzo, A. A., Orme, I. M., Almo, S. C., Leyh, T. S., and Chan, J. (2009) *Mycobacterium tuberculosis* universal stress protein Rv2623 regulates bacillary growth by ATP-binding: requirement for establishing chronic persistent infection. *PLoS Pathog. 5*, e1000460.
10. Kvint, K., Nachin, L., Diez, A., and Nystrom, T. (2003) The bacterial universal stress protein: function and regulation. *Curr. Opin. Microbiol. 6*, 140–145.
11. Sousa, M. C., and McKay, D. B. (2001) Structure of the universal stress protein of *Haemophilus influenzae*. *Structure 9*, 1135–1141.
12. O'Toole, R., and Williams, H. D. (2003) Universal stress proteins and *Mycobacterium tuberculosis*. *Res. Microbiol. 154*, 387–392.
13. Kelly, D. J., and Thomas, G. H. (2001) The tripartite ATP-independent periplasmic (TRAP) transporters of bacteria and archaea. *FEMS Microbiol. Rev. 25*, 405–424.
14. Galinski, E. A., and Herzog, R. M. (1990) The role of trehalose as a substitute for nitrogen-containing compatible solutes (*Ectothiorhodospira halochloris*). *Arch. Microbiol. 153*, 607–613.
15. Kunte, H. J., and Galinski, E. A. (1995) Transposon mutagenesis in halophilic eubacteria: conjugal transfer and insertion of transposon Tn5 and Tn1732 in *Halomonas elongata*. *FEMS Microbiol. Lett. 128*, 293–299.
16. Studier, F. W. (2005) Protein production by auto-induction in high density shaking cultures. *Protein Expression Purif. 41*, 207–234.
17. Kabsch, W. (1993) Automatic processing of rotation diffraction data from crystals of initially unknown symmetry and cell constants. *J. Appl. Crystallogr. 26*, 795–800.
18. McCoy, A. J. (2007) Solving structures of protein complexes by molecular replacement with Phaser. *Acta Crystallogr., Sect. D: Biol. Crystallogr. 63*, 32–41.
19. CCP4 (1994) The CCP4 suite: programs for protein crystallography. *Acta Crystallogr., Sect. D: Biol. Crystallogr. 50*, 760–763.
20. Cohen, S. X., Morris, R. J., Fernandez, F. J., Ben Jelloul, M., Kakaris, M., Parthasarathy, V., Lamzin, V. S., Kleywegt, G. J., and Perrakis, A. (2004) Towards complete validated models in the next generation of ARP/wARP. *Acta Crystallogr., Sect. D: Biol. Crystallogr. 60*, 2222–2229.

21. Murshudov, G. N., Vagin, A. A., and Dodson, E. J. (1997) Refinement of macromolecular structures by the maximum-likelihood method. *Acta Crystallogr., Sect. D: Biol. Crystallogr. 53*, 240–255.
22. Painter, J., and Merritt, E. A. (2005) A molecular viewer for the analysis of TLS rigid-body motion in macromolecules. *Acta Crystallogr., Sect. D: Biol. Crystallogr. 61*, 465–471.
23. DeLano, W. L. The PyMOL Molecular Graphics System, Delano Scientific LLC, San Carlos, CA (http://www/pymol.org).
24. Holm, L. S. (1997) Dali/FSSP classification of three-dimensional protein folds. *Nucleic Acids Res. 25*, 231–234.
25. Notredame, C., Higgins, D. G., and Heringa, J. (2000) T-Coffee: a novel method for fast and accurate multiple sequence alignment. *J. Mol. Biol. 302*, 205–217.
26. Altschul, S. F., Gish, W., Miller, W., Myers, E. W., and Lipman, D. J. (1990) Basic local alignment search tool. *J. Mol. Biol. 215*, 403–410.
27. Thompson, J. D., Higgins, D. G., and Gibson, T. J. (1994) CLUSTAL W: improving the sensitivity of progressive multiple sequence alignments through sequence weighting, position specific gap penalties and weight matrix choice. *Nucleic Acids Res. 22*, 4673–4680.
28. Hall, T. A. (1999) BioEdit: a user-friendly biological sequence alignment editor and analysis program for Windows 95/98/NT. *Nucleic Acid Symp. Ser. 41*, 95–98.
29. Gouet, P., Robert, X., and Courcelle, E. (2003) ESPript/ENDscript: extracting and rendering sequence and 3D information from atomic structures of proteins. *Nucleic Acids Res. 31*, 3320–3323.
30. Mushegian, A. R., and Koonin, E. V. (1996) Sequence analysis of eukaryotic developmental proteins: ancient and novel domains. *Genetics 144*, 817–828.
31. Zarembinski, T. I., Hung, L. W., Mueller-Dieckmann, H. J., Kim, K. K., Yokota, H., Kim, R., and Kim, S. H. (1998) Structure-based assignment of the biochemical function of a hypothetical protein: a test case of structural genomics. *Proc. Natl. Acad. Sci. U.S.A. 95*, 15189–15193.
32. Ogura, T., Whiteheart, S. W., and Wilkinson, A. J. (2004) Conserved arginine residues implicated in ATP hydrolysis, nucleotide-sensing, and inter-subunit interactions in AAA and AAA+ ATPases. *J. Struct. Biol. 146*, 106–112.
33. Scheffzek, K., Ahmadian, M. R., Kabsch, W., Wiesmuller, L., Lautwein, A., Schmitz, F., and Wittinghofer, A. (1997) The Ras-RasGAP complex: structural basis for GTPase activation and its loss in oncogenic Ras mutants. *Science 277*, 333–338.
34. Gauthier, M. J., Lafay, B., Christen, R., Fernandez, L., Acquaviva, M., Bonin, P., and Bertrand, J. C. (1992) *Marinobacter hydrocarbonoclasticus* gen. nov., sp. nov., a new, extremely halotolerant, hydrocarbon-degrading marine bacterium. *Int. J. Syst. Bacteriol. 42*, 568–576.
35. Kuhlmann, S. I., Terwisscha van Scheltinga, A. C., Bienert, R., Kunte, H. J., and Ziegler, C. (2008) 1.55 Å structure of the ectoine binding protein TeaA of the osmoregulated TRAP-transporter TeaABC from *Halomonas elongata*. *Biochemistry 47*, 9475–9485.
36. Lecher, J., Pittelkow, M., Zobel, S., Bursy, J., Bonig, T., Smits, S. H. J., Schmitt, L., and Bremer, E. (2009) The crystal structure of UehA in complex with ectoine—a comparison with other TRAP-T binding proteins. *J. Mol. Biol. 389*, 58–73.
37. Saum, S. H., Sydow, J. F., Palm, P., Pfeiffer, F., Oesterhelt, D., and Muller, V. (2006) Biochemical and molecular characterization of the biosynthesis of glutamine and glutamate, two major compatible solutes in the moderately halophilic bacterium *Halobacillus halophilus*. *J. Bacteriol. 188*, 6808–6815.
38. Diederichs, K., and Karplus, P. A. (1997) Improved R-factors for diffraction data analysis in macromolecular crystallography. *Nat. Struct. Biol. 4*, 269–275.